Table I. Comparison of the anomalous photoemission peak with observed low-energy characteristic energy-loss peaks. E_a refers to the energy of the anomalous peak with respect to the Fermi level, E_{d1} to the highest-energy d-band photoemissive peak, and ΔE_1 to the lowest energy-loss peak. All energies are in eV.

Metal	E_a	E_{d1}	$E_{d1}-E_a$	ΔE_1
Fe	-5.5^a	-0.3^a	5.2	5.3 ± 0.4^c
Co	-5.1^a	-0.3^a	4.8	4.6 ± 0.4^c
Ni	-4.6^a	-0.3^a	4.3	4.3 ± 0.4^c
Cu	-6.2^b	-2.1^b	4.1	4.5 ± 0.2^c
Ag	$<-7.0^b$	-4.2^b	>2.8	4.1 ± 0.1^d
Pd	$\sim-7.0?^a$	-0.2^a	6.8	6.8 ± 0.2^d

[a]A. Y.-C. Yu and W. E. Spicer, Phys. Rev. Letters 17, 1171 (1966) (see especially Ref. 11).

[b]W. E. Spicer, in Optical Properties and Electronic Structure of Metals and Alloys, edited by F. Abelès (John Wiley & Sons, Inc., New York, 1966), pp. 296-315.

[c]J. L. Robins and J. B. Swan, Proc. Phys. Soc. (London) 76, 857 (1960).

[d]J. L. Robins, Proc. Phys. Soc (London 78, 1177 (1961).

effect and not a lowered plasma loss. Although photoemission data do not extend to this energy, Yu and Spicer[1] indicate the presence of an optical reflectivity peak at −7.0 eV and do not rule out the possibility of a photoemission peak at this energy.

It should be emphasized that our proposed explanation of the observed anomalous peaks does not attribute them directly to the electronic density of states. On physical grounds, we argue that such peaks should occur as a consequence of energy loss to secondary excitations, and therefore that the observed "optical" density of states should correspond qualitatively to the result of folding the characteristic loss spectrum into the true density of states. The relative magnitude of these secondary peaks depends on the strength of interactions that are not directly related to the true density of states. This is compatible with the observed wide variation of the relative strength of the anomalous peaks in different transition metals.[1]

The authors are indebted to Professor W. E. Spicer for several valuable discussions.

[1]C. N. Berglund and W. E. Spicer, Phys. Rev. 136, A1044 (1964); A. J. Blodgett, Jr., and W. E. Spicer, Phys. Rev. 146, 390 (1966); Phys. Rev. Letters 15, 29 (1965). W. E. Spicer, J. Appl. Phys. 37, 947 (1966); A. Y.-C. Yu and W. E. Spicer, Phys. Rev. Letters 17, 1171 (1966). W. E. Spicer, in Optical Properties and Electronic Structure of Metals and Alloys, edited by F. Abelès (John Wiley & Sons, Inc., New York, 1966), pp. 296-315; C. N. Berglund, ibid., pp. 285-295.

[2]J. C. Phillips, Phys. Rev. 140, A1254 (1965).

[3]J. R. Cuthill, A. J. McAlister, and M. L. Williams, Phys. Rev. Letters 16, 993 (1966).

[4]H. D. Hagstrum and G. E. Becker, Phys. Rev. Letters 16, 230 (1966).

[5]S. J. Nettel, Phys. Rev. 150, 421 (1966).

[6]M. H. El Naby, Z. Physik 174, 269 (1963); H. Mayer and M. H. El Naby, Z. Physik 174, 189, 280 (1963); H. Mayer and B. Hietel, in Optical Properties and Electronic Structure of Metals and Alloys, edited by F. Abelès, (John Wiley & Sons, Inc., New York, 1966), pp. 47-59.

[7]R. A. Ferrell, in Optical Properties and Electronic Structure of Metals and Alloys, edited by F. Abelès (John Wiley & Sons, Inc., New York, 1966), pp. 78-82.

[8]F. S. Ham, Phys. Rev. 128, 82 (1962).

[9]J. Dickey, Phys. Rev. 81, 612 (1951); S. Methfessel, Helv. Phys. Acta 31, 303 (1958).

[10]C. N. Berglund and W. E. Spicer, Phys. Rev. 136, A1030 (1964).

[11]J. L. Robins and J. B. Swan, Proc. Phys. Soc. (London) 76, 857 (1960).

[12]J. L. Robins, Proc. Phys. Soc. (London) 78, 1177 (1961).

DIRECT ELECTROMAGNETIC GENERATION OF ACOUSTIC WAVES*

J. R. Houck,† H. V. Bohm,‡ B. W. Maxfield, and J. W. Wilkins§
Laboratory of Atomic and Solid State Physics and Department of Physics, Cornell University, Ithaca, New York
(Received 21 June 1967)

A recent Letter by Larsen and Saermark[1] describes the electromagnetic generation of acoustic waves in aluminum. They explain their experimental results on the basis of the helicon-phonon interaction. The present paper presents evidence that rf-ultrasonic coupling can occur near the surface of a metal in the presence of a magnetic field, independent of helicon propagation. The results of our experiments are consistent with a model which assumes that the external electromagnetic fields couple directly with the electromagnetic fields of the acoustic wave.

The experimental arrangement is shown in

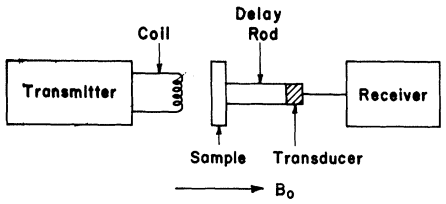

FIG. 1. The sound wave generated by an rf pulse in the coil propagates through the sample and the 3-cm-long X-cut quartz delay rod to the 10-MHz AC-cut quartz transducer. The experiment was performed at 4.2°K in a 50-kG superconducting solenoid.

Fig. 1. The rf fields generated by the coil excite an acoustic wave at the surface of the sample. The acoustic wave is detected by a piezoelectric transducer after propagating through the sample and the quartz delay rod. The pulsed electronics system is similar to that used in conventional ultrasonics.

We have studied a number of samples using a 1-μsec burst of 10-MHz carrier; carrier frequencies up to 40 MHz were briefly surveyed. We have found it possible to excite an ultrasonic signal in the sample by pulsing the rf coil and using the quartz transducer as a receiver (the quartz delay rod is used to obtain a time separation of several microseconds between the transmitted pulse and the received signal). Conversely, the electromagnetic fields of a sound wave generated in sample by the quartz transducer induced a voltage in the coil. The amplitude of the transmitted ultrasonic signal was found to be proportional to the magnetic strength. In general, the signal-to-noise ratio was less than 2 for $B_0 < 5$ kG.

The effect can be seen most simply be treating the metal as a two-component plasma of electrons and ions. Let n (N) be the number density and m (M) the mass of the electrons (ions) of charge $-e$ ($+Ze$). In aluminum, the square of the electron plasma frequency $\omega_p^2 (= 4\pi ne^2/m)$ and of the ion plasma frequency $\Omega_p^2 (= 4\pi Z^2 Ne^2/M = 4\pi nZe^2/M)$ are 5.6×10^{32} sec^{-2} and 3.6×10^{28} sec^{-2}, respectively. The cyclotron frequency ω_c [$= eB_0/(mc)$] at 10 kG is 1.8×10^{11}. A characteristic transverse sound velocity s is 3.4×10^5 cm/sec in Al and a typical frequency of the applied ac field is 10^7 Hz. Take the static field B_0 in the z direction; use the $\pm$ notation (e.g., $E^\pm = E_x \pm iE_y$) for all transverse fields and currents. Then the Fourier components in space (k) and time (ω) of the ionic and electronic currents can be written as

$$4\pi i\omega J_{\text{ion}}^{\pm} = -\frac{\omega\Omega_p^2}{\omega^2 - s^2k^2}E^{\pm} \tag{1}$$

and

$$4\pi i\omega J_{\text{el}}^{\pm} = \mp\frac{\omega\omega_p^2}{\omega_c}E^{\pm}. \tag{2}$$

In the expression for the electronic current we have supposed, for simplicity, that $\omega_c\tau \gg 1$, $\omega\tau$, or $v_F k\tau$, where τ is relaxation time of electrons and v_F is the Fermi velocity. Furthermore, we have neglected Shubnikov–de Haas effect in electrical conductivity. Likewise for simplicity (and not necessity) we have neglected the attenuation of the acoustic waves.

These two equations must be consistent with Maxwell's equations and boundary conditions at the surfaces. For simplicity we circumvent the boundary value problems by a self-consistent treatment of the electric field. That is, we write $E = E_{\text{ext}} + E_{\text{ind}}$, where E_{ext} is the externally applied ac electric field of the coil and E_{ind} is the field induced by the currents via Maxwell's equations. Hence, in the low-frequency limit, the wave equation becomes

$$4\pi i\omega J^{\pm} = c^2k^2E_{\text{ind}}^{\pm}, \tag{3}$$

where $J^{\pm} = J_{\text{ion}}^{\pm} + J_{\text{el}}^{\pm}$.

Solving for the ionic current, we find that

$$4\pi i J_{\text{ion}}^{\pm} = \frac{\omega_p^2c^2k^2}{D_{\pm}(k,\omega)}E_{\text{ext}}^{\pm}.$$

The denominator

$$D_{\pm}(k,\omega) = (s^2k^2 - \omega^2)(c^2k^2 \pm \omega\omega_p^2/\omega_c) - \omega^2\Omega_p^2$$

has poles at

$$s^2k_{\pm}^2 \cong \mp\left(\frac{s^2\omega_p^2\omega}{c^2\omega_c} + \frac{\Omega_p^2\omega\omega_c}{\omega_p^2}\right), \quad \text{"heliconlike"} \tag{4a}$$

$$\cong \omega^2 \pm (\Omega_p/\omega_p)^2\omega\omega_c, \quad \text{"acoustic."} \tag{4b}$$

The poles (4a) correspond to helicon (k_-) and the damped wave (k_+) of opposite helicity. The shift in the helicon wave vector due to the ions is less than 0.01%. The effect of the electrons on the acoustic poles (4b) is much larger and is demonstrated most clearly by calculating the residue of the ionic current at the acous-

Table I. Materials in which electromagnetically generated acoustic waves have been observed.

Sample	Structure	Thickness, d (mm)	Remarks
Ag	110	6.3	$d \gg \lambda_{\text{sound}}$
Al	110	3.0	$d \gg \lambda_{\text{sound}}$
	111	4.5	
	Polycrystalline foil	0.02	$d \ll \lambda_{\text{sound}}$
PbTe	100	2.1	$V_{\text{sound}} \approx V_{\text{helicon}}$

tic poles (4b):

$$4\pi i \operatorname{Res}(J_{\text{ion}}^{\pm}(k_{\pm}^2)) \simeq \pm\left[\frac{c\Omega_p k_{\pm}}{s\omega_p}\right]^2 \omega_c E_{\text{ext}}^{\pm}.$$

Hence, the coupling of the ionic current to the applied electric field (E_{ext}) is linear in the static magnetic field as observed.

In a field of 10 kG, a 10-MHz helicon would not propagate because of damping via the mechanism of Doppler-shifted cyclotron resonance absorption. This form of nonlocal damping occurs when $kv_F > \omega_c$, which is never the case for the acoustic poles for the range of frequencies and static magnetic fields used in this experiment.

Since the time delay of the transmitted ultrasonic signal does not vary (within a measurement accuracy of approximately 2%) as a function of magnetic field, and because the ultrasonic signals may be seen below the magnetic field strength of the "helicon edge," it is evident that the interaction is not dependent upon the generation of helicon waves in the conventional sense. Further, the amplitude of the ultrasonic signals does not change significantly when the sample is tilted with respect to the magnetic field up to an angle of approximately 15° (the largest angle for which data have been obtained).

Table I gives a brief summary of our observations. The measured transit times through aluminum agree well with previous measurements.[2] To date we have not investigated in detail the parameters governing the generation of various types of ultrasound. For example, in the aluminum-foil sample we found that the only signal received by the quartz transducer was a slow shear wave in the quartz delay rod ($v_S \approx 3.2 \times 10^5$ cm/sec), whereas as in the [111] single-crystal aluminum sample we have observed the sound velocity in the quartz delay rod to be the fast shear wave ($v_S \approx 5.1 \times 10^5$ cm/sec). We have also received signals using an X-cut (i.e., longitudinal wave) quartz transducer; it is, however, very possible that these signals were due to mode conversion at various boundaries. Theoretical considerations suggest that both shear modes and possibly the longitudinal mode may be generated in the sample. The detection of these various modes depends strongly upon the relative orientation of metal sample (if it is a single crystal), the delay rod, and the shear axis of the quartz transducer.

The amplitude of the signal produced in the single-crystal aluminum samples (resistivity ratio of 5000) displayed the usual Landau-level oscillations for $B_0 \gtrsim 25$ kG. The periods of these oscillations are in agreement with the known Fermi surface of aluminum. The amplitude of the oscillations increased as the temperature was reduced to 2°K.

In the metal samples, the phase velocity of the sound wave is much greater than the helicon phase velocity; thus the two modes are essentially independent.[3] However, the helicon and sound-wave velocities are nearly equal in the PbTe sample, and hence there is a strong mixing of the two modes. The observed signals were qualitatively different in the case of PbTe. The pulse amplitude was not linearly related to B_0, and there were indications that there was acoustic generation throughout the bulk of the sample.

It is a pleasure to thank Professor N. W. Ashcroft for many stimulating discussions.

*This work was supported in part by the U. S. Atomic Energy Commission Contract No. AT(30-1)-2150, NYO-2150-30, in part by U. S. Office of Naval Research under Contract No. NONR-401(38), Technical Report No. 21, and in part by the Advanced Research

Projects Agency through the Materials Science Center at Cornell University, Report No. MSC-706.

†Present address: Center for Radio Physics and Space Research, Cornell University, Ithaca, New York.

‡Permanent address: Department of Physics, Wayne State University, Detroit, Michigan.

§Alfred P. Sloan Foundation Fellow.

[1]P. K. Larsen and K. Saermark, Phys. Letters 24A, 374, 668 (1967). Similar observations have been made in bismuth: V. F. Gantmakher and V. T. Dolgopolov, Zh. Eksperim. i Teor. Fiz.—Pis'ma Redakt. 5, 17 (1967) [translation: JETP Letters 5, 12 (1967)].

[2]G. N. Kamm and G. A. Alers, J. Appl. Phys. 35, 327 (1964).

[3]One of us, JRH, has studied the propagation of helicon pulses in metallic sodium (to be published).

THERMOMAGNETIC EFFECTS IN SUPERCONDUCTING NIOBIUM†

A. T. Fiory* and B. Serin
Department of Physics, Rutgers, The State University, New Brunswick, New Jersey
(Received 2 June 1967)

The observations of a Peltier effect[1] and an Ettingshausen effect[2] in type-II superconductors in the flux-flow state have been explained in terms of the motion of individual fluxoids by the original authors and in subsequent, more detailed treatments.[3-5] We wish to report detailed observations of both effects in pure niobium, which cannot be explained in terms of a simple fluxoid model, and which moreover suggest that in the flux-flow state the normal current makes a contribution to the entropy flow.

This investigation was made possible by Dr. R. W. Meyerhoff of the Union Carbide Corporation,[6] who provided us with a specimen of pure niobium with a ratio of 3000 between the room-temperature resistance and the value at 9.5°K. The specimen was in the form of a strip 2.5 cm long by 0.52 cm wide by 0.02 cm thick. A uniform magnetic field could be applied perpendicular to the plane of the strip. The specimen was clamped at its ends to current leads of high electrical conductance made of a slightly impure indium alloy, and these leads were in the normal state at all temperatures at which measurements were made. All the data were taken with a current density of 1330 A/cm^2. Quantities measured in the direction of current flow will be given a subscript x, while those transverse to the current will be denoted with a subscript y.

Carbon resistance thermometers and Constantan heaters of matched resistance were mounted at each end of the specimen at the In-Nb junctions. With current flowing, the power dissipated in the heater at the cold junction was adjusted so that the thermometer readings were unchanged when the current direction was reversed and the power moved to the opposite junction. This power equals twice the Peltier power. The temperature difference across the specimen never exceeded a few millidegrees. The Peltier power was divided by the current to yield the usually defined Peltier coefficient,[7,8] Π_x. We estimate the relative accuracy of the values of Π_x in the flux-flow state to be better than 5%.

Thermometers were also mounted on each edge of the specimen at its center, and the temperature difference ΔT_y determined for each current direction. Appropriate power was dissipated in the heaters at the ends to nullify the effects of Peltier heat. The thermal conductivity of the specimen, κ, was also measured as a function of magnetic field[9] while the current was flowing through it. Instead of the Ettingshausen coefficient,[7] we define a quantity $\Pi_y = -(\Delta T_y)\kappa/wJ_x$, where w is the width of the specimen and J_x the current density, which is the analog of Π_x. The relative accuracy of these measurements is estimated to be 10%.

In addition, appropriately placed probes permitted the longitudinal voltage (see Fig. 3) developed across the specimen to be measured, as well as the Hall voltage near each junction. The two Hall voltages so determined were averaged to allow for slightly different behavior at each junction. The voltages were converted to a longitudinal electric field, E_x, and a Hall field, E_y. These data are similar to those published[10] for niobium. We remark that between about $0.95H_{c2}$ and H_{c2} both electric fields show a relatively rapid increase compared to their rates of change at lower magnetic fields.